Accepted Manuscript

Interrogating the Dimerization Interface of the Prion Protein Via Site-Specific Mutations to p-Benzoyl-L-Phenylalanine

Sudheer Babu Sangeetham, Krisztina Huszár, Petra Bencsura, Antal Nyeste, Éva Hunyadi-Gulyás, Elfrieda Fodor, Ervin Welker

PII: S0022-2836(18)30451-0
DOI: doi:10.1016/j.jmb.2018.05.027
Reference: YJMBI 65735

To appear in:

Received date: 3 February 2018
Revised date: 7 May 2018
Accepted date: 14 May 2018

Please cite this article as: Sudheer Babu Sangeetham, Krisztina Huszár, Petra Bencsura, Antal Nyeste, Éva Hunyadi-Gulyás, Elfrieda Fodor, Ervin Welker , Interrogating the Dimerization Interface of the Prion Protein Via Site-Specific Mutations to p-Benzoyl-L-Phenylalanine. The address for the corresponding author was captured as affiliation for all authors. Please check if appropriate. Yjmbi(2018), doi:10.1016/j.jmb.2018.05.027

Interrogating the dimerization interface of the prion protein via site-specific mutations to *p*-benzoyl-L-phenylalanine

Sudheer Babu Sangeetham[1], Krisztina Huszár[2], Petra Bencsura[2], Antal Nyeste[1,3], Éva Hunyadi-Gulyás[1], Elfrieda Fodor[1,¶], Ervin Welker[1,2¶]

[1]Institute of Biochemistry, Biological Research Center, Hungarian Academy of Sciences, Szeged, Hungary

[2]Research Centre for Natural Sciences, Hungarian Academy of Sciences, Budapest, Hungary

[3]ProteoScientia Ltd., Cserhátszentiván, Hungary

[¶] These authors contributed equally to this work.

Correspondence should be addressed to Ervin Welker: Institute of Biochemistry, Biological Research Centre, HAS, Temesvari krt 62, H-6726, Szeged, Hungary. Tel: +36-62-599631, e-mail: welker.ervin@brc.mta.hu

Running title: Site-specific photo-crosslinking of prion protein dimers

[1]

[1] ***Abbreviations***: *p*Bpa, *p*-benzoyl-L-phenylalanine; PrP, prion protein; mPrP, mouse prion protein; mPrPmch, mouse prion protein fusion with mCherry; PrP^{C}, cellular prion protein ; PrP^{Sc}, Scrapie prion; HD, hydrophobic domain; CR, central region; OR, octarepeat region; GPI, glycophosphatidyl-inositol; PBS , phosphate buffer saline; aa, amino acid; WT, wild type.

Abstract

Transmissible spongiform encephalopathies are centered on the conformational transition of the prion protein from a mainly helical, monomeric structure to a β-sheet rich ordered aggregate. Experiments indicate that the main infectious and toxic species in this process are however shorter oligomers, formation of which from the monomers is yet enigmatic. Here, we created 25 variants of the mouse prion protein site-specifically containing one genetically-incorporated *p*ara-benzoyl-phenylalanine (*p*Bpa), a cross-linkable non-natural amino acid, in order to interrogate the interface of a prion protein-dimer, which might lie on the pathway of oligomerization. Our results reveal that the N-terminal part of the prion protein, especially regions around position 127 and 107, is integral part of the dimer interface. These together with additional *bb*Bpa-containing variants of mPrP might also facilitate to gain more structural insights into oligomeric and fibrillar prion protein species including the pathological variants.

Keywords: prion; dimerization; photo-crosslinking; *p*Bpa; protein conformational stability

Introduction

While the exact physiological function of the prion protein (PrP) is not fully understood, it seems to be a promiscuous protein being involved in several cellular processes and interacting with a great number of partners [1–8]. Nevertheless, PrP is famous for its involvement in devastating neurodegenerative disorders, especially in transmissible spongiform encephalopathies (TSEs), a group of incurable and lethal diseases [9,10]. In most of the cases, the origin of TSE is unknown (sporadic), but in some instances familial or infectious origins can be revealed in the history of the patients. Although the pathologies of various TSEs are slightly different depending on the origins of the diseases and on the area of the brain that is first affected, the fundamental event is the conformational transition of the normal, cellular prion protein (PrP^{C}) of the host to an aggregated β-sheet-rich state (PrP^{Sc}) [9–12] . The difference between the two states of PrP is purely conformational and both forms are glycosylated, equipped with a GPI anchor and are stabilized by one intramolecular disulfide bond [13–28].

The pathways of PrP^{C} to PrP^{Sc} formation are not clear and the fact that PrP can form several different type of oligomeric, aggregated or fibrillar states makes it no simpler to discern. A number of conversion reactions have been established using brain-derived mammalian PrP^{C} or even bacterially expressed recombinant PrP, revealing several features of the conversion, the formed proteinase K (PK)-resistant or infectious material and the necessary co-factors [29–43]. However, much less understood are the initial steps leading to dimer and/or oligomer formation and their relation to fibril formations.

The spontaneous formation of PrP^{Sc} from wild type PrP^{C} and its leading to a self-sustainable process might occur in extremely rare instances, if at all, in the genesis of sporadic TSE.

Spontaneous formation occurs more frequently in familial TSEs [44,45]. Enhancing the spontaneous *in vitro* bbconversion of PrP to forms reminiscent, at least in some aspects, of PrP^{Sc} is generally attempted by destabilizing the conformation of the recombinant PrP using chemicals and/or varying the pH or the temperature [32,46–52]. Reduction of the disulfide bond destabilizes the protein [53,54] and also potentiates the conversion of PrP to oligomeric forms [49,54,55]. These β-sheet rich misfolded oligomers, while exhibiting some low level PK-resistance, likely have different structures from those of brain-derived PrP^{Sc} that possesses an intact disulfide bond [14,15]. Several forms of oligomers with different structures and sizes can be prepared and even oligomers with different characteristics generated under identical conditions have been described [46,56–61]. Some of these PrP oligomers generated *in vitro* are cytotoxic to cells and are thought to lay off the pathways of fibril formations [46,62,63]. However, it is not clear that which if any of them are the toxic and/or infectious species formed during the course of TSE. It is also not clear if the starting point of oligomerization is a monomeric or a dimeric form.

Interestingly, a number of studies employing various approaches suggested that a fraction of PrP^{C} exist as alpha helical dimers in vivo [64–67] and pointed to the importance of dimerization in the physiological functions and cytoprotective roles played by PrP^{C} (reviewed by [68]). In-cell dimerization of PrP^{C} in cell lines and primary neurons increases trafficking to the plasma membrane and production of the neuroprotective metabolites of PrP, PrPN1 [69,70] and PrPC1 [71], and of shed-PrP [72], which also led to the proposition of an alternate, dimerization-regulated secretion pathway for PrP^{C} that would allow a quick response to toxic stimuli [73]. The hydrophobic domain (HD) of PrP was proven to be essential for the α-cleavage to occur [74], the mechanism that produces these protective metabolites. Using N2a cells it was also demonstrated that the HD (aa 112 to 133) of mouse

PrP, is essential for the dimerization of PrP, as well as that a PrP^{C} dimer is essential for the toxicity of PrP^{Sc} [67].

An alpha helical dimer is also formed from recombinant Syrian hamster PrP, fragment 90 to 231[PrP(90-231)] with low SDS concentration [75]. However, it was not clear if it represents a native form or it is already a species/intermediate in the conversion of PrP [76,77]. The formation of PrP^{C} dimer may be critical at the strat of PrP misfolding, which at first, may or may not involve the partial unfolding of the protein.

Here, we developed a system for the creation of PrP variants each bearing one cross-linkable, genetically coded unnatural amino acid substitution at predetermined positions. This tool may facilitate the identification of "true" PrP interactors/binding partners in vivo under well-defined conditions, as well as to map the structure of the pathological form of PrP and interrogate the conformation of the intermediate/dimeric PrP species. Here, we used this tool to investigate the dimerization surface of an alpha helical PrP dimer.

Results

The series of site specific *p*Bpa-mutant prion proteins generated to map the dimerization site of the mouse prion protein and tagged by mCherry

We adapted the system developed by the Schultz laboratory [78] for genetic incorporation of unnatural amino acids into protein sequences in *Escherichia coli* (*E. coli*) for the purpose to produce *p*Bpa-mutants of the mouse prion protein (mPrP). This system is based on a cognate tRNA and amino acyl synthetase pair orthogonal to the *E. coli* machinery and is capable of introducing para-benzoylphenylalanine (*p*Bpa) to amber stop codons.

In order to facilitate generation of *p*Bpa-point mutants sweeping through regions of interest in the sequence, we introduced new unique restriction sites to the coding sequence of PrP by silent mutations. These, allowed later for the introduction of amber codon mutations by simple linker ligation along the almost entire coding region of mPrP (see Materials and Methods). Using such an approach ensured an easy access to the great number (about 50 from which 38 are used here) of mutant PrPs we generated.

For the position of *p*Bpa insertion, we aimed to cover also regions that were previously proposed to be involved in dimerization/oligomerization, such as the hydrophobic domain (HD, residues 111 to 134) [67,73,79] or the central region (CR, residues 105 to 125) [80] or the N-terminal 90-120 segment [81], and also few positions that are not considered to be taking part in the dimerization surface. With this strategy we selected a set of 24 positions, with 20 falling in the N-terminal half and HD and additional two positions in the C-terminal half of the protein (Fig. 1a).

After initial experiments, owning to its higher expression levels with *p*Bpa analogs, we generated amber stop codon mutants of mPrP in fusion with an mCherry fluorescent protein

expression cassette at the C-terminus using pRSET-B vectors for expression. The tag allowed on the one hand, visual examination and tracking of the protein during purification steps, aiding optimization of the conditions, and on the other hand, might slightly increase the solubility and promote easier handling of the protein. Later, we also generated untagged PrP constructs for *p*Bpa substitutions at selected positions, and tested the untagged mPrPs also to verify whether the tag may have any significant influence on the results obtained.

The purified wild type (WT) and *p*Bpa-mutant PrP-mCherry fusion proteins appear at about the same position on SDS polyacrylamide gels and at around their expected molecular weights of 52 kDa, constituted by the MW of PrP (23.1 kDa) and of the mCherry tag (29 kDa) (Fig. 1b).

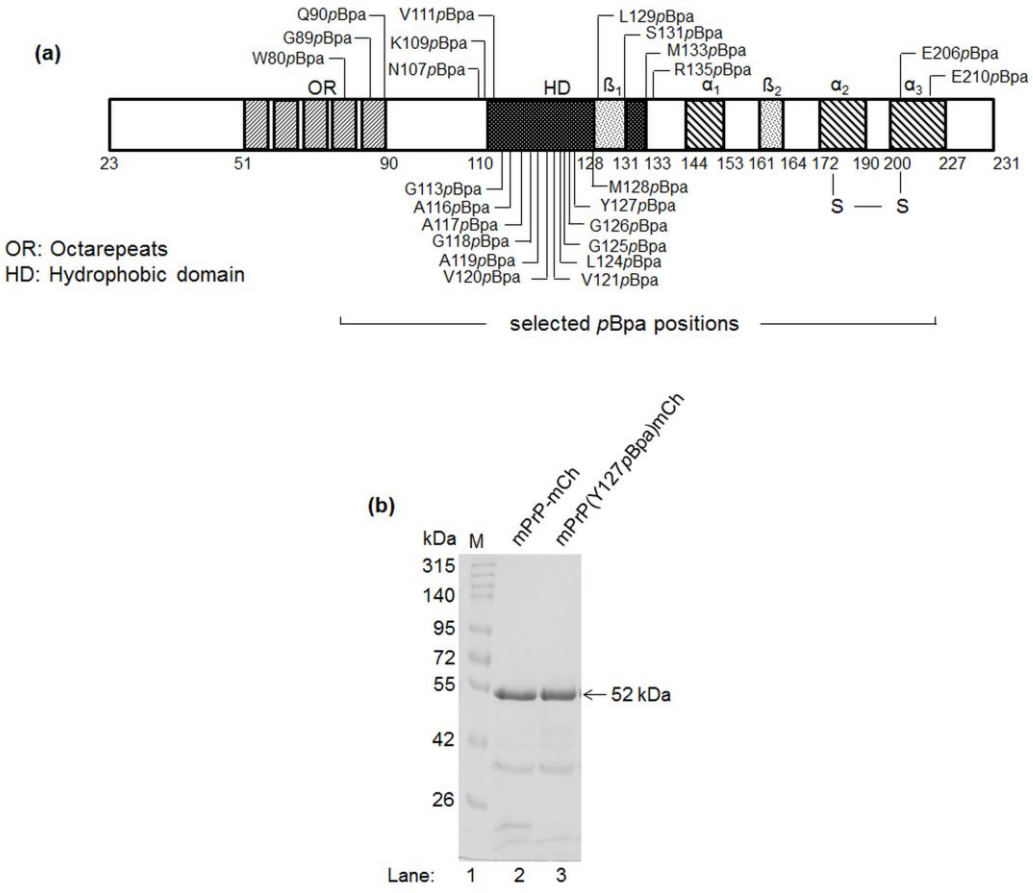

Fig. 1. The series of site specific single-*p*Bpa-mutant PrPs generated. (a) Schematic diagram of the mPrP sequence (aa 23-231) indicating the residues chosen for *p*Bpa-mutation to generate a series of single-*p*Bpa-mutant mPrPs, and the structural features of the protein, (β_1 and β_2: beta sheets, $\alpha_{1\text{-}3}$: alpha helices, S-S: disulfide bond). (b) Representative SDS-PAGE of purified mCherry tagged wild type (lane 2, mPrPmCh) and a *p*Bpa-mutant [lane 3, mPrP(Y127*p*Bpa)mCh] prion protein on a 10% polyacrylamide-SDS gel. Proteins resolve at about their expected weights, sum of wtPrP and mCherry (~52 kDa). Additional bands can be observed below the full length protein, common for mCherry-tagged proteins, due to the hydrolysis of the acylimine linkage of the chromophore of mCherry upon sample-treatment such as SDS-denaturing and boiling, and fragmentation of the mCherry during SDS-PAGE analysis [82–85].

We found best protein yields when using LB media as contrast to minimal media for culturing. It has been reported that the amino acyl synthetase might retain some of its ability to charge its cognate tRNA with tyrosine, especially when the protein is expressed in LB medium. To see if insertion of *p*Bpa indeed occurred selectively, we cultured and induced in parallel cells transfected by the wild type protein gene, the protein gene containing the amber codon at a desired position (here at codon 131) and a mutant protein coding for a tyrosine at that position. All three cultures were either supplemented by *p*Bpa or were grown without *p*Bpa and were induced for protein expression. The purified proteins were excised from SDS gels and analyzed by mass spectrometry (for details see Materials and Methods). The results confirmed that a correctly inserted *p*Bpa is present in at least ~90% in the produced *p*Bpa-mutant protein samples and insertion occurred only at the expected position (Fig. S1).

_p_Bpa insertions did not affect protein conformational stabilities

With a few exceptions, we placed most of the *p*Bpa substitutions, in the conformationally disordered part of the prion protein, where this is not expected to result in structural changes of the folded protein and alterations in protein stability. However, to test for such possible effects, we performed stability tests on selected mutants and the wild type protein, using an urea gradient assay developed for disulfide bond containing proteins [86]. In this assay, the disulfide-containing protein is being treated by increasing concentrations of urea in the presence of a low concentration of reducing agent (here 20 mM DTT). As the urea unfolds the protein, the disulfide bonds became available to the reducing agent and can be reduced, whereas this can not take place if the protein is still folded. By blocking the reducing agent and the protein thiols at this time (e.g. by applying NEM in excess) the folded (and disulfide-

intact) and unfolded (reduced) protein populations present in the sample can be fixed and later be visualized on non-reducing SDS-polyacrylamide gel based on the differing mobilities of the disulfide-intact and reduced forms. In the case of the prion protein, there are two cysteines that form one disulfide bond within the C-terminal globular half of the protein stabilizing its structure. Since, the mCherry does not possess internal cysteines, the method is applicable for testing not only the untagged PrP, but also the prion-mCherry fusion constructs: the unfolding of mCherry being silent in this assay, does not yield change in the mobility on a denaturing gel. Also, without a functional interaction between PrP and mCherry, the unfolding of mCherry is not expected to affect the stability of the prion protein's structure /unfolding process. In line with this, the gradual appearance of the unfolded prion proteins at increasing urea concentrations can be clearly detected (Fig. 2).

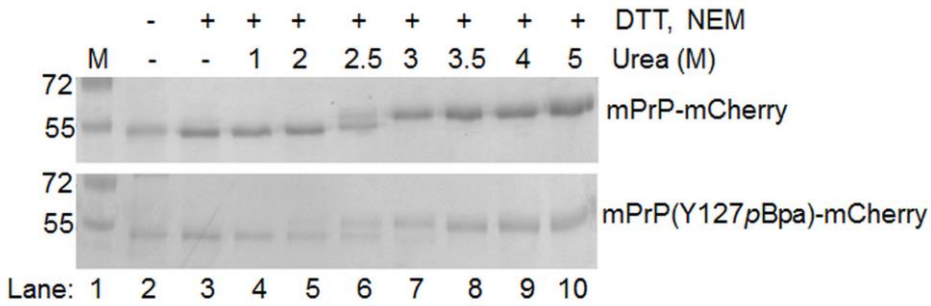

Fig. 2. The WT and *p*Bpa-mutant prion-mCherry proteins have similar conformational stabilities. Representative gel pictures of the urea gradient assay for WT and 127*p*Bpa mutant, as indicated on the figure.

Along with the WT, several mutant variants were tested: positions 127, 128 and 129 that might be part of the C-terminal globular domain (aa 125-227) of the bacterially expressed prion protein [87,88] and are also reported to be part of or adjacent to protein-protein interaction regions [89]. We also chose two *p*Bpa substitutions at positions Glu206 and

Glu210 that are part of the helix III of PrP. We found that the proteins with *p*Bpa substitutions have similar unfolding patterns as the wild type protein; their transition regions are within 2 to 4 M urea, and midpoints at 3 ± 0.5 M urea concentration (Fig. S2). These indicate that substitutions of amino acids at these positions to *p*Bpa did not perturb the stability of the protein and also suggest that *p*Bpa can be well-tolerated in these protein structures.

The mCherry-tagged prion proteins harboring site specific mutations to photo-sensitive *p*Bpa successfully crosslink a dimeric complex when photo-activated in a dimeric state

The purified recombinant prion protein is known to be prone to oligomerize in solutions around physiological pH [46,59,90], a phenomenon that is also concentration dependent [50,91] Kaimann et al. [76] had shown that by applying different submicellar concentrations of SDS in the buffer, the recombinant hamster prion protein (haPrP 90-231) could be kept in specific oligomeric states, dimeric or higher oligomeric, depending on the amount of SDS applied. Based on their findings we optimized the conditions of photo-crosslinking reactions for both sample condition and the parameters of the UV-crosslinking. Applying 0.06% SDS in PBS buffer of pH 7.4 and a protein concentration of 6 µM we could achieve successful crosslinks of dimeric proteins that are demonstrated (Fig. S3) on reducing SDS-polyacrylamide gels. To exclude the possibility to account for dimers that crosslinked through a non-*p*Bpa residue (a process the prion protein prone to) two types of controls were present in all experiments: non-irradiated samples, which had been incubated in dark and the wild type protein, which has been irradiated, both for the very same length of time as the experimental samples. Careful handling and timely processing of the samples kept minimal the appearance of non-*p*Bpa crosslinked protein species on the SDS gels. According to this

protocol, each purified *p*Bpa-mutant prion-mCherry fusion protein, a total of 24 and the wild type, were irradiated and were tested for the appearance of photo-crosslinked dimers by SDS-PAGE (Fig. 3).

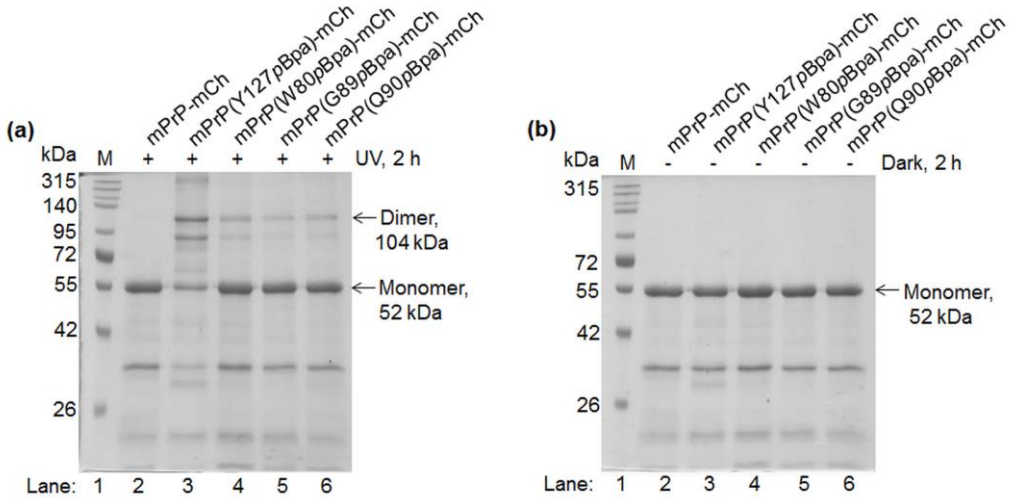

Fig. 3. Photo-crosslinking of dimers of various prion-mCherry proteins containing site specifically inserted *p*Bpa in the sequence of the PrP. Representative pictures of reducing 10% polyacrylamide gels of WT and selected *p*Bpa-mutants (a) irradiated at 365 nm for 2 h and (b) non-irradiated, but incubated at dark in otherwise similar conditions as indicated on the figure. Proteins are crosslinked at 6 µM concentration in the presence of 0.06% SDS (in PBS, pH 7.4) that favors its dimerization. For optimization of SDS concentration and irradiation time see Fig. S3 and S4, respectively.

The appearance of the crosslinked dimer can be observed at the expected molecular weight of around 104 kDa -the double of the monomeric protein weight of 52 kDa, both marked by arrows (lanes 3 through 6 on Fig. 3a). There are no bands present at above the monomeric sizes for the WT (no *p*Bpa-containing) and for the non-irradiated (lane 2 on Fig. 3a and 3b,

respectively) samples, suggesting that all bands appearing in this region for the irradiated samples correspond to crosslinked proteins. The two characteristic satellite bands for the crosslinked samples observable between dimeric and the monomeric forms and for all samples below the monomeric form, are not the results of proteolytic degradation but of the specific cleavage of mCherry taking place in the sample buffer as mentioned earlier. To ensure the proper interpretation of samples showing minimal or no specific crosslinking, a positive control (*p*Bpa mutant at position 127) was included in all experiments.

As expected, the amount of crosslinked dimers differs for different positions of *p*Bpa, reaching highest level for the variant containing *p*Bpa at position 127. However, we can not entirely exclude the possibility that some amount of dimers or oligomers apparent on the gels originate from nonspecific association of protein molecules that were locked in the irradiated samples by *p*Bpa crosslinking.

The amount of non-specific dimers crosslinked

To be able to measure the true dimer-crosslinking efficiency, we need to account for any nonspecific dimers that result from random, temporary association of the two protein molecules that may be crosslinked by *p*Bpa during irradiation. To solve this problem we chose to look for conditions that move the system away from the dimer specific equilibrium and effectively disrupt the specific interactions that could result in dimer formation. We experimented with increasing the concentration of SDS to find conditions in which the protein is in monomeric state. This could be well indicated by the gradual disappearance of the dimer band of the most efficiently crosslinking sample, the Y127*p*Bpa mutant, after irradiation. While testing a range of SDS concentrations between 0.2 to 5% (Fig. S4), we found that above 2% SDS the amount of crosslinked dimer in the irradiated sample was not decreasing

anymore. Therefore, we performed the crosslinking experiments side-by-side at 0.06% and 2% SDS conditions (Fig. 4 and Fig. S6), for each particular position (i.e. mutant), to assess for the amount of nonspecifically crosslinked product. We considered the crosslinked dimeric complexes at 2% SDS as being the maximal fraction of unspecific background arising from capturing random associations.

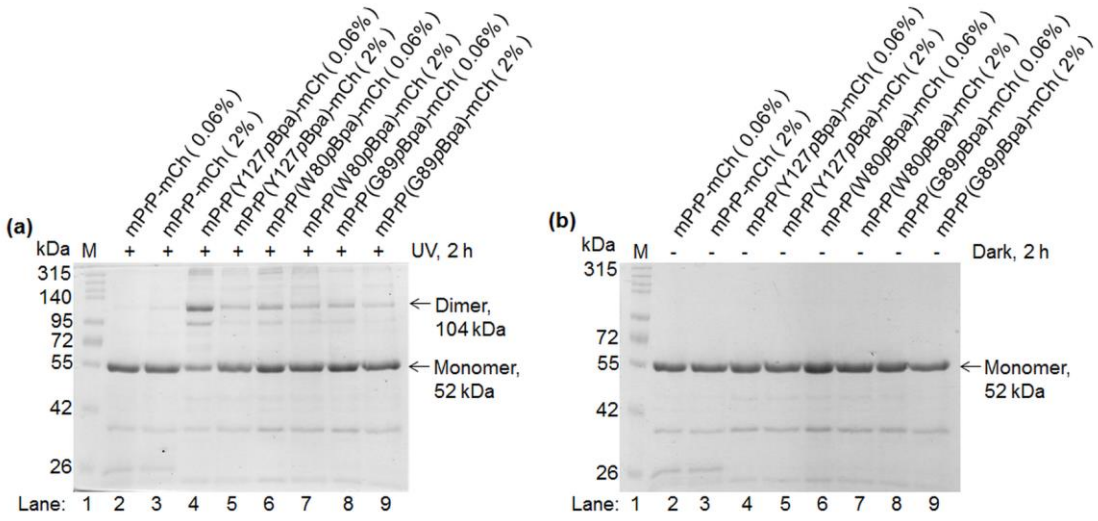

Fig. 4. Assessing the specific and nonspecific dimers crosslinked. Representative gel pictures of WT and selected *p*Bpa-mutant prion-mCherry proteins as indicated, irradiated at 365 nm (a) or kept at dark (b) for 2 h, at dimer (0.06%) or monomer (2%) favoring SDS conditions. (The value of 2% for SDS was chosen based on Fig. S5. For the rest of the 24 positional *p*Bpa-mutants see Fig. S6).

Discerning the residue positions involved in the dimerization interface during specific dimer interactions of PrP-mCherry through estimating crosslinking efficiencies.

The efficiencies of various positional *p*Bpa-mutants to crosslink PrP dimers at 0.06% SDS were calculated based on gel-densitometry analysis of the SDS-PAGE of crosslinked proteins (presented on Fig. 3, 4 and S6) as described in Materials and Methods, and it is shown on Fig. 5.

(a)

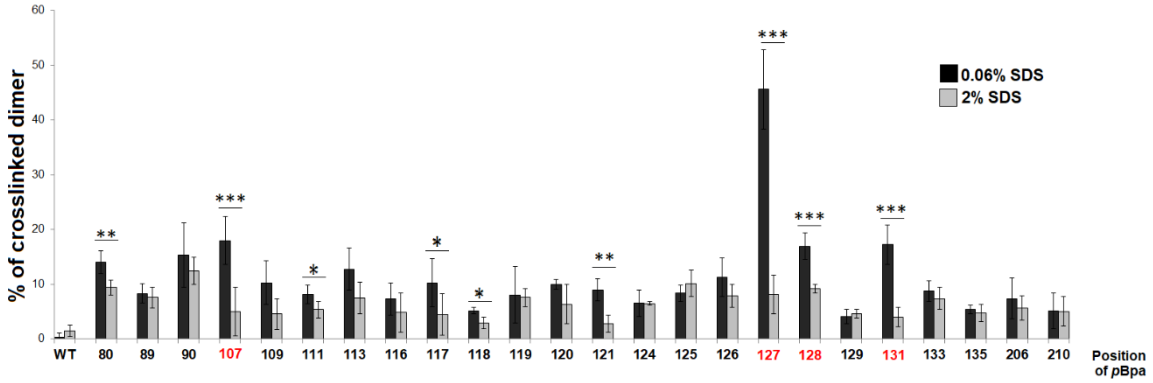

(b)

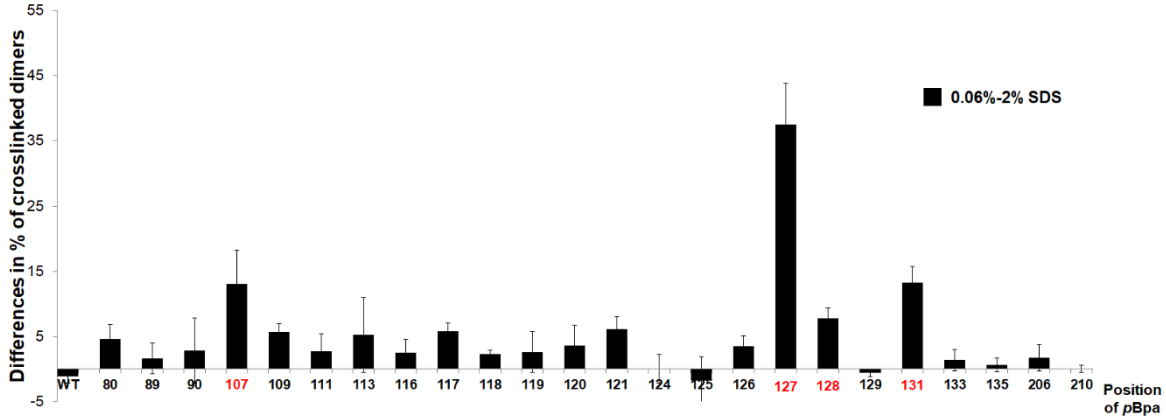

(c)

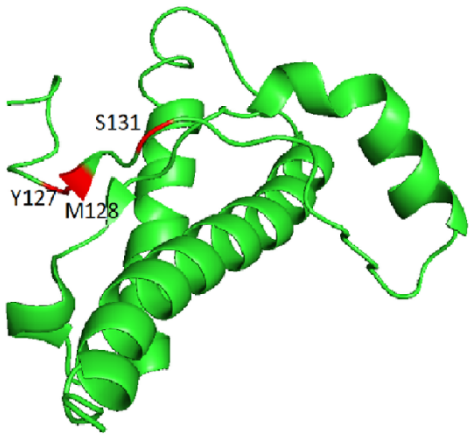

Fig. 5. Efficiencies of crosslinking specific dimers of PrP by positional variants of *p*Bpa mutant prion-mCherry proteins. Percentages of crosslinked dimers are shown (a) for various *p*Bpa positional mutants obtained under conditions that either favors dimerization (0.06% SDS, black bars) or rather a monomeric state (2% SDS, grey bars). Dimer percentages were evaluated by gel-densitometry analysis as described in Materials and Methods and error bars show the standard deviations from mean of repeated experiments. For each protein, the difference between the values obtained in dimer-specific and non-dimer specific conditions (0.06% SDS and 2% SDS) was calculated (b) and was tested for significance using Student's t-test. The significant differences that are marked on (a) were considered as those positions where specific dimer-crosslinking occured. Asterisks indicate as follows: *: $p<0.05$, **: $p<0.01$, ***: $p<0.001$. A three dimensional ribbon diagram of the mPrP for the available sequence region 120-230 aa. is shown on panel (c) with the most significant dimer-crosslinker positions (127, 128, 131) highlighted along the sequence on the 3D fold. Position 107 also has significant dimer crosslinking efficiency but falls outside of this fold.

The highest efficiency of crosslinking the dimer was obtained for the position of 127 of the *p*Bpa that resulted about 40% crosslinked protein amount. This was followed by position 131, 107 and 128, respectively, yielding between 10% and 20% crosslinked products. Altogether, 9 out of the 24 positions examined resulted crosslinked protein amounts significantly higher than that corresponding to non-specific association of the proteins in 2% SDS.

Untagged prion protein mutants with site specifically inserted *p*Bpa efficiently crosslink dimeric complexes at conditions favoring dimer formation.

After successful optimization of the expression of *p*Bpa-containing tagged prion protein variants, to check if the presence of mCherry tag had any influence on the dimerization of the prion proteins, we engineered a selected set of 14 pRSETB expression plasmids with amber codon-mutant untagged mouse prion protein DNAs and using similar conditions produced the untagged proteins. We selected positions for amber codon placement based on the results of Fig. 5, namely positions 80, 90, 107, 111, 113, 116, 119, 120, 121, 124, 127, 128, 129 and 131, representing both efficient and inefficient dimer-crosslinking. The purified recombinant untagged prion and *p*Bpa-mutant prion proteins show single bands on reducing SDS-PAGE gels at the expected molecular weights of 23 kDa (Fig. 6a).

Similarly, to mCherry-tagged variants, we tested the stabilities of the untagged WT and *p*Bpa-mutant prion proteins by urea gradient assay. Comparing the WT and the mPrP(Y127*p*Bpa) mutant, we found same transition regions of between 2 to 3 M urea, and same transition midpoint at around 2.5 M for both proteins (Fig. 6b).

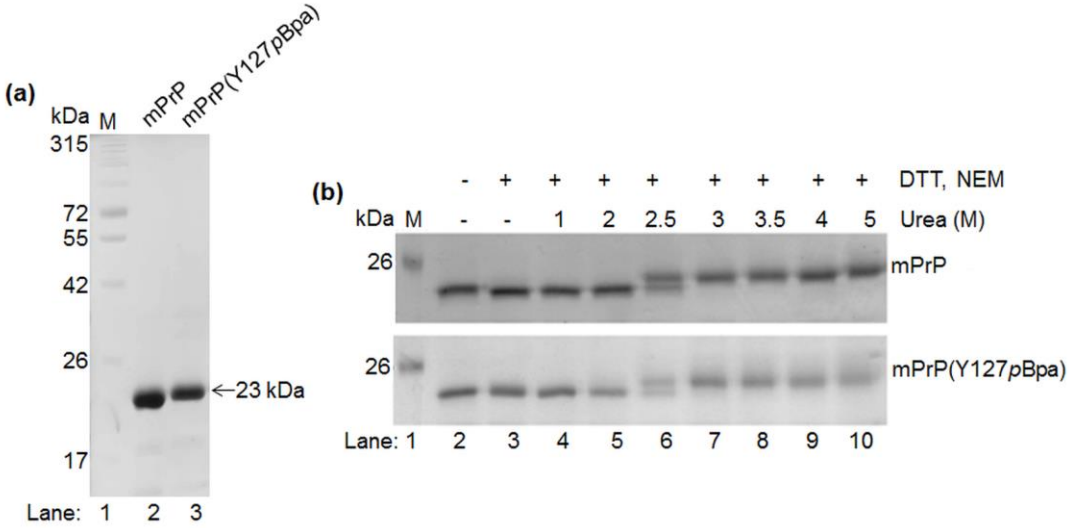

Fig. 6. Untagged wild type and *p*Bpa-mutant PrPs have similar conformational stabilties. Representative pictures of 12% polyacrylamide-SDS gels: (a) the purified WT and *p*Bpa-mutant proteins and (b) the urea gradient assays as indicated on the figure.

We performed crosslinking experiments with the untagged WT and *p*Bpa-mutant PrPs in same conditions as forthe mCherry-tagged versions of the proteins: at 0.06% and 2% SDS conditions (in PBS, pH 7.4) favoring dimer and monomer formation of PrP, respectively, and tested the samples similarly on reducing SDS-gels. After irradiation, for *p*Bpa-mutant protein samples a crosslinked population can be observed at the expected molecular weight of a dimer (Fig. 7a), at ~46 kDa. Also, higher molecular weight bands can be seen, indicative of low quantities of trimeric and tetrameric complexes of ~69 and ~92 kDa, respectively. In the case of the control samples that were kept at dark in parallel, no dimers can be observed (Fig. 7b).

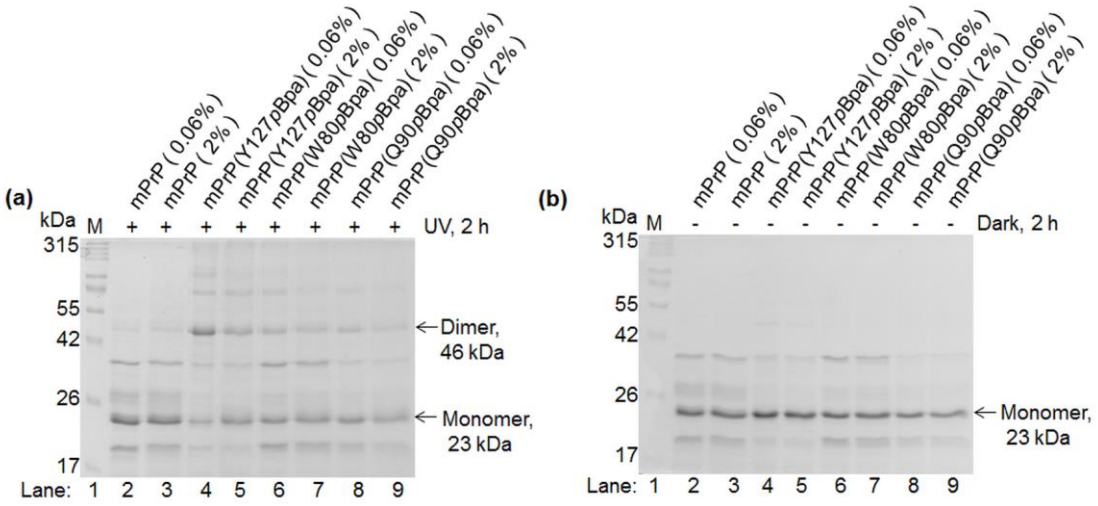

Fig. 7. Non-specific crosslinked dimers. Representative pictures of reducing 12% polyacrylamide gels of selected proteins bearing *p*Bpa-mutations**.** (a) Samples irradiated at

365 nm for 2 h. (b) non-irradiated samples, incubated in the same conditions at dark as indicated in the figure. Proteins (6 µM) are crosslinked side-by-side in the presence of either 0.06% or 2% SDS (in PBS, pH 7.4), conditions that favor either dimerization or the monomeric form of the prion protein, respectively. For the additional *p*Bpa-mutants tested see Fig. S7.

Efficiencies of dimer crosslinking were evaluated as previously, considering the sum of dimer and monomeric bands as 100%, both at 0.06% and at 2% SDS conditions, and by correcting for the controls (Fig. 8).

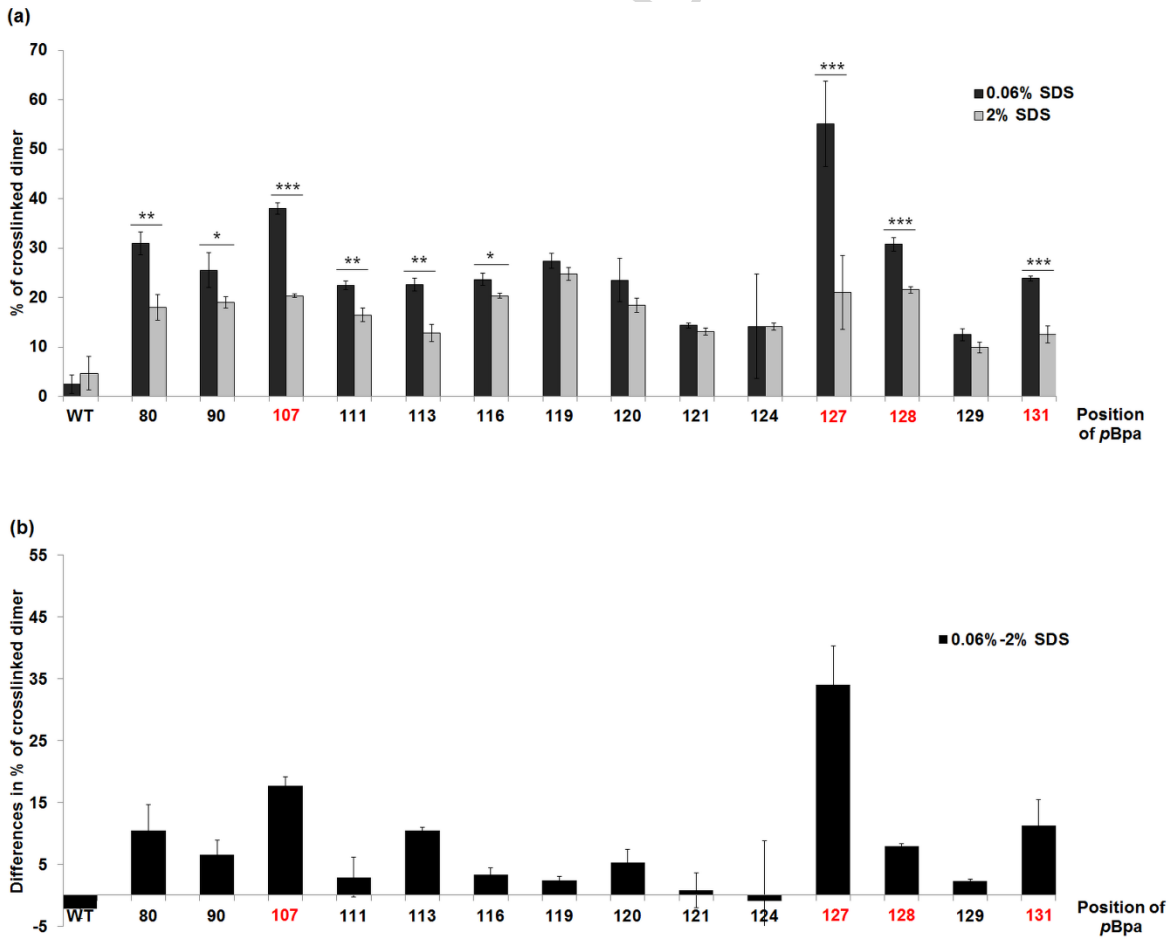

Fig. 8. Positional variants of untagged *p*Bpa-mutant prion proteins efficiently crosslink dimer complexes. Bars represent (a) crosslinked dimer-percentages obtained for *p*Bpa-mutants under conditions that either favor dimerization (0.06% SDS, black bars) or rather a monomeric state (2% SDS, grey bars) as calculated in Fig. 5 and (b) their differences (2% SDS-subtracted-values). Values on (a) represent averages obtained for at least 4 repetitions of the experiment and error bars show the standard deviations from mean. Significant differences between the 0.06 and 2% SDS results were assessed by Student's t-test and are indicate for corresponding positions on panel (a) by asterisks as follows *: $p<0.05$, **: $p<0.01$, ***: $p<0.001$.

The highest amounts of dimers could be crosslinked when *p*Bpa is inserted at position 127, yielding almost 40% crosslinked dimers above the unspecific control 2% SDS condition, similarly as in case of mCherry-tagged set of proteins. The positional mutants 107, 113, 128 and 131 are among those showing the highest efficiencies, as in case of the mCherry tagged proteins. Eight out of the 14 mutants examined exhibited significant amount of crosslinked products above those found in the monomeric, 2% SDS, condition.

These data indicate that the same positional *p*Bpa-mutants provide efficient dimer-crosslinking in both tagged and untagged froms and that the *p*Bpa-mutants have generally similar ranking irrespective of being tagged by mCherry or untagged.

Finally, we also recorded circular dichroism (CD) spectra of the WT and the mutant proteins under conditions that favor either monomer or dimer PrP to look for secondary structural element rearrangements (Fig. S8). On the one hand, we confirmed our earlier results (Fig. 2, Fig. 6b and supplementary Fig. S2) that the mutations do not perturb significantly the native

structure of WT-PrP. On the other hand, we found that there are little variations in the CD spectra of the prion proteins between monomer and dimer favoring condition; PrP, in line with earlier studies [72,73] preserves its overall helical fold under dimerization.

Discussion

In studies preceding this work, a dimer with mainly α-helical structure was identified and discussed as an intermediate on the putative pathway from the PrP^C to the pathogenic form [75,76]. These earlier studies were carried out using recombinant hamster PrP (90–231) arguing that this represents the amino acid sequence of infectious prion rods, or PrP 27–30, and contains only the rigid part of the structure. Here, we used the full length recombinant mouse PrP (aa 23-231) to approximate better the physiological fold of the protein, either tagged by an mCherry at the C-terminal or untagged, to interrogate the structure of PrP.

Unlike earlier studies, we used *p*Bpa, a site specific crosslinker that reacts with C-H groups of the protein backbone and side chains when they are within a distance of less than 3.1 A° from *p*Bpa in a protein structure. By contrast, when flexible parts of a complex are crosslinked, methionine may mediate efficient crosslinking up to a distance of 13 A° referred to as magnet effect of methionine [92–94]. The 90-135 segment of PrP is thought to possess some flexibility in PrP monomers and likely, in a dimer too; in the solution NMR structure only the 124-135 region is structured. Thus, many of the positions containing *p*Bpa substitutions here may lie in the flexible region making them prone to interact with a nearby active methionine. However, the flexible 23-124 fragment has no methionine, which substantially decreases the likeliness of such an unspecific methionine "magnet effect" [93].

*p*Bpa when placed at the beginning of the structured domain of PrP, positions 126-131, confers highest propensity for crosslinking the dimer (with 127 *p*Bpa being the most efficient), suggesting that this region is either part of or neighbour the dimer interface. Earlier studies have shown that a Cys131 mutant of overexpressed mouse PrP^C forms disulfide-bonded dimer in the membrane of SH-SY5Y human neuroblastoma cells, suggesting that position 131 is part of or is close to the interface of the dimer and also that a homodimeric interface is formed [67]. Our results are in line with these observations supporting the notion that the PrP^C dimers formed in the cell membrane of mammalian cells under more physiological condition and *in vitro* in 0.06% SDS share structural features.

Several positions in the flexible tail of PrP between 80 and 126 containing *p*Bpa mediate dimer crosslinking to a lesser but significant extent. Positions (107, 111, 113) with high specificity crosslinkings mark the beginning of the HD region. By contrast, positions in the HD region itself show lesser crosslinks, 5 positions examined with the untagged protein exhibit no specific crosslinkings. Since the *p*Bpa mutation in position at the interface might interfere with the binding, more efficient *p*Bpa crosslinkings might occur at region neighboring the actual binding site as it is apparent here. Thus, this observation is consistent with a picture where the HD region is involved in dimer formation by forming a homodimeric interface. Interestingly, the Tatzel's lab reported that in the absence of the HD region the disulfide dimer of PrP involving Cys131 was not formed underlining the essential role of the HD region in dimer formation [67].

Additionally to the protein segment involving the HD region, we also investigated PrP variants containing *p*Bpa at either position 89 or 90. The results showing specific crosslinking with both variants corroborate earlier works from the Riesner lab using similar experimental conditions (0.06% SDS, pH 7.2) but recombinant hamster 90-231 PrP, where the N-terminal amino group of Gly90 is crosslinked to Glu152, or Glu196 or Asp202 in both the dimer and

monomeric protein [75,76]. The specificity of the interactions towards three out of the many acidic side chains of the protein indicates that the N-terminus of the recombinant protein is constrained at least to one side of the PrP fold of the protein and at the same time the very N-terminal parts reserved some conformational freedom. Molecular modelling using some of these experimental constrains resulted in a structure where the 90-124 tail acquires stabile structural features and folds back along the 128-152 segment forming the homodimeric interface of the dimer [75,76]. Our results showing interaction sites along the whole 90-125 segment is consistent with this structure and establishes a link between the dimer observed with prion proteins anchored to the plasma membrane of mammalian cells and dimer observed with the recombinant prion protein *in vitro* 0.06% SDS. The *p*Bpa-containing PrP variants as well as the methods established here, among other approaches may potentiate the direct testing of whether the dimer observed here is on the pathways of oligomerisation, fibrillization and possibly of the formation of PrP^{Sc}, by triggering the process from the covalently crosslinked dimer forms.

In conclusion, our results show that the N-terminal flexible tail, approximately between 90 and 124 aa of PrP, acquires some stabile, structurally constrained conformations in the dimer formed at low SDS concentration *in vitro* and, similarly to the dimer formed in the mammalian cell membrane, likely forms a homodimeric interface involving at least parts of the HD. The methodology established here provides an easy access to non-natural amino acid-containing PrP variants and, in combination with mass spectrometry analysis, could also facilitate mapping the interface of PrP molecules in PrP^{Sc} and in amyloid PrP preparations.

Materials and Methods

DNA cloning and plasmid constructs

DNA oligos were obtained from Microsynth AG (Austria). The correct sequences for the expression cassettes in all plasmids generated in this study were confirmed by Sanger sequencing (Microsynth AG). All plasmids were constructed with standard molecular biology techniques, briefly as follows.

Cloning of pET22b-PrP and pET41-PrP plasmids

The cDNA of mouse PrP (mPrP) (Uniprot entry P04925) was from the Caughey lab [95]. Bacterial expression plasmid vectors pET22b and pET41 (Merck Millipore) and preparation of the pET22b-PrP and pET41-PrP plasmids was carried out as follows. The DNA fragments encoding the wild type (mPrP) or 3F4-epitope- harbouring (mPrP3F4) mPrP [96] (aa 23-231), preceded by a methionine in case of pET41-PrP vectors and followed by a cysteine and a stop codon for both vectors, were amplified by PCR with the following primers: *pET22b-PrP5* and *pET22b-PrP3 or pET41-PrP5* and *pET41-PrP3* respectively (for sequences see Table S1). The methionine, cysteine and stop codons were introduced into the amplicons with the respective PCR primers. The PCR fragments were purified using Nucleospin Gel and PCR Clean-up Kit (MACHEREY-NAGEL) after agarose gel electrophoretic separation and the purified DNA fragments were digested overnight by EcoRI (pET22b) or by NdeI and HindIII (pET41). The 5' end of the pET22b insert was left uncut. In case of vector pET22b the prepared PCR fragments were inserted between the MscI and EcoRI restriction sites of the plasmid after the PelB signal. In case of vector pET41 the prepared PCR fragments were inserted between the NdeI and HindIII sites of the plasmid.

The insertion of tyrosine (Tyr) or Amber stop (Amb) codons into the coding sequence of mPrP encoded by the pET41-PrP plasmids was carried out by QuikChange site directed mutagenesis. The Tyr or Amber codons (denoted by: *) were inserted at the 5' or 3' side of

the mPrP's KKRPK motif, resulting in the following variants of both mPrP and mPrP3F4: MYKKRPK (Tyr inserted before KKRPK) and M*KKRPK (Amber before KKRPK) or KKRPKY (Tyr after KKRPK) and KKRPK* (Amber after KKRPK). The mutagenesis primers were the following, in the respective order of the constructs above: *petmutMYKfwd, petmutMYKrev, petmutMAmbKfwd, petmutMAmbKrev, KKRPKYfwd, KKRPKYrev, KKRPKAmbfwd, KKRPKAmbrev*. (For oligonucleotide sequences see Table S1).

Cloning of the pRSET-B expression vectors

Bacterial expression plasmid vector pRSETB was obtained from Thermo Fisher Scientific. For the sequences of the oligonucleotides used for PCR and linker ligation (Table S2). The nucleic acid sequences of the bacterial expression vectors pRSETB-mPrP and pRSETB-mPrP-mCh and the amino acid sequences of the proteins encoded by them: the full length mouse prion protein followed by a cysteine residue and in the second case by an mCherry fusion tag, 6xHis and a Cys (referred to in short as the wild type untagged and the wild type tagged mPrP proteins, in order to contrast their corresponding amber codon mutants, in the text), can be found in **Supplementary Data**, respectively.

The pRSETB-mPrP and pRSETB-mPrP-mCh plasmids were used also as parental plasmid vectors for generating the amber stop codon mutants : pRSETB-mPrP(S131X), pRSETB-mPrP(E206X), pRSETB-mPrP(E210X), where the numbers denote the positions of mutations to amber codon (noted as X) in respect to the full length sequence of mPrP protein including the signal sequences 1-23. Mutations were carried out by QuikChange site directed mutagenesis with the following primers: *mPrPS131Ambfwd, mPrPS131Ambrev, PrP-E206X-fw, PrP-E206X-rev, PrP-E210X-fw* and *PrP-E210X-rev*, respectively.

The vectors pRSETB-mPrP-RE and pRSETB-mPrP-mCh-RE were generated from pRSETB-mPrP and pRSETB-mPrP-mCh vectors for cloning purposes, by the introduction of

unique restriction enzyme sites (EagI, BsmBI and MluI) at strategic positions into the prion protein coding sequence using QuikChange site directed mutagenesis. The DNA oligonucleotide primers used for the silent mutagenesis were, in respective order of the introduced restriction sites shown above: *EagIfwd, EagIrev, BsmBIfwd, BsmBIrev, MluIfwd, MluIrev.*

The following mutations were introduced into the sequence of mPrP encoded by the pRSETB-mPrP-RE and pRSETB-mPrP-mCh-RE vectors: W80X, G89X, Q90X, N107X, K109X, V111X, G113X, A116X, A117X, G118X, A119X, V120X, V121X, L124X, G125X, G126X, Y127X, M128X, L129X, M133X or R135X. The mutations were introduced to both plasmids by linker ligations using the linkers (Table S3). The procedure was carried out briefly, as follows.

The pRSETB-mPrP-RE and pRSETB-mPrP-mCh-RE plasmids were digested with the appropriate restriction endonulease pairs for each mutant (Table S3 for mutations and respective restriction endonuclease pairs), purified with NucleoSpin DNA purification kit, (MACHEREY-NAGEL) and the appropriate DNA linker or linkers were ligated between the two sticky ends of the plasmid (Table S3; for the oligonucleotides making up the DNA linkers, Table S2). When a fragment of the prion protein coding sequence was reconstituted from two or more linkers, all 5' termini of the oligonucleotides at the linker junctions were phosphorylated.

Expression and purification of proteins

Recombinant wild type and *p*Bpa-mutant prion proteins with and without an mCherry fusion tag were produced in *E. coli* BL-21(DE3) protein expression strain based on published

protocols for wild type [97] and for site-specific incorporation of *p*Bpa into proteins for the *p*Bpa-mutants [98], as follows.

For the wild type proteins the pRSETB expression plasmids carrying the mPrP or mPrP-mCherry genes (pRSETB-mPrP and pRSETB-mPrP-mCh) were transfected into competent *E.coli* BL21(DE3) cells, and transformant cells were selected on Luria-Bertani (LB) agar plates in presence of 100 μg/ml ampicillin. In case of the *p*Bpa-mutant proteins, first the pEVOL-pBpF plasmid [99] expressing the cognate tRNA and the amino acyl transferases and possessing a chloramphenicol resistance gene, was transfected into competent *E.coli* BL21(DE3) cells. This plasmid was kindly provided by the laboratory of P. Schultz (The Scripps Res. Inst.) Transformant cells were selected on LB-agar plates in presence of 34 μg/ml chloramphenicol and competent cells were prepared by $CaCl_2$ method [100]. These pre-transformed cells were used in the second step to transfect the pRSETB-expression plasmids harboring the amber codon mutant-prion genes of interest and possessing an ampicillin resistance gene. Successful transformants were selected on LB-agar plates in presence of both of the antibiotics, ampicillin: 100 μg/ml and chloramphenicol: 34 μg /ml, and were used to produce the recombinant proteins, as follows. For both WT and *p*Bpa-mutant protein expressions, single colonies were picked from the selection plates to inoculate starter cultures of 50 ml LB media, which were grown overnight at 37 °C in presence of the corresponding antibiotics, ampicillin 50 μg/ml or both ampicillin and chloramphenicol (50 μg/ml and 17 μg/ml, respectively). Volumes of 600 ml LB media with the corresponding antibiotics were inoculated from the starter cultures to yield 0.01 OD_{600} density and were cultured further at 37 °C under high aeration (in Erlenmeyer beakers of two liters and agitation at 280 rpm). When the density reached 0.5-0.6 $O.D_{600}$ the cultures were induced for protein expression: for the wild type proteins IPTG (Thermo Fisher Scientific) was added at a

0.9 mM final concentration, for the *p*Bpa-mutant proteins (also the Tyr-mutant and wild type mPrPmCherry proteins used for mass spectrometry verification of *p*Bpa insertion) both 0.9 mM IPTG and 0.02% L-arabinose (Sigma-Aldrich) were added and also 1 mM *p*Bpa (BACHEM) (freshly dissolved in 1 M NaOH) was supplemented to the culture at this time. The induced cultures were further grown typically for four hours at 37 °C, or ten hours at 28 °C (we found no substantial difference in yield between the two conditions). Longer culture times at 37 °C for the mCherry tagged proteins resulted harvested bacterial pellets with colorless halo–indicative of the absence of mCherry and likewise the absence of protein expression as well, a condition that served us as a marker for optimizing the time length of the growth. Cells were harvested by centrifugation at 2704 x g for 15 min at 4 °C, and were resuspended in 100 mM NaCl supplemented with 0.5 mM PMSF (Sigma-Aldrich), 1x concentration of Protease Inhibitor Cocktail (Sigma-Aldrich). The bacterial cells were disrupted on ice by sonication (Sonifier Cell Disruptor B-30, Branson Sonic Power Co, USA) applying a 30 s on- and 30 s off-pulse repeated for seven times, and the lysate was centrifuged at 60,480 x g for 50 min at 4 °C. The insoluble inclusion bodies, containing the proteins of interest sedimented in the pellet, were collected and solubilized in 30 ml of Buffer A: 6 M Gn-HCl (Alfa Aesar (Thermo Fisher Scientific)), 10 mM Tris, 100 mM Na_2HPO_4-$2H_2O$, pH 8.0, for 1 h by stirring on ice. After centrifugation (60,480 x g, 50 min, 4 °C) the supernatant was applied to Ni-NTA agarose (MACHEREY-NAGEL) of 3 ml bed-volume pre-equilibrated by buffer A, and the suspension was gently mixed on a rocker for 30 minutes on ice to allow binding of the proteins to the Ni-NTA beads. The suspension was sedimented by centrifugation (750 x g, 3 min, 4 °C) and the pelleted beads were washed two times using buffer B: 1 M GnHCl, 10 mM Tris, 100 mM $Na_2HPO_4.2H_2O$, pH 8.0, and centrifugation at 750 x g for 3 min at 4 °C. Next, a redox buffer: 1 M GnHCl, 10 mM Tris, 100 mM $Na_2HPO_4.2H_2O$, 0.5 mM PMSF, 1x concentration of Protease Inhibitor Cocktail, 5 mM

GSSG (Sigma-Aldrich), 10 mM GSH (Sigma-Aldrich), pH 8.0, was added to the pelleted beads and the suspension was kept on ice while gently mixing on a rocker for ~16 h to refold the prion protein [101,102]. The refolded protein-bead suspension was poured onto an empty column. The flow through was kept to test for the presence of unbound proteins, and the beads were washed by using 75 ml of washing buffer: 10 mM Tris, 100 mM $Na_2HPO_4.2H_2O$, 20 mM imidazole (Sigma-Aldrich), pH 5.8. The proteins were eluted by elution buffer: 10 mM Tris, 100 mM $Na_2HPO_4.2H_2O$, 500 mM imidazole, pH 5.8 collecting about 6 fractions of 1 ml. Fractions collected were tested for the presence of protein of interest using SDS-PAGE with ProSieve QuadColor prestained protein marker (Lonza) and those containing most of the protein were pooled together and were dialyzed in dialysis buffer: 20 mM CH3COONa, pH 5.5, at 1:1000 excess volume for about 18 h at 4 °C with three changes. Dialyzed proteins were tested on SDS-PAGE their concentration was measured by Bradford method [103] and the yield of the protein expression was estimated. Aliquots of 1 mL of the dialyzed proteins were flash-frozen by liquid nitrogen and were stored at -80 °C for later use.

Mass spectrometry analysis of *p*Bpa insertion into proteins

For mass spectrometry analysis all protein samples were run on 10% polyacrylamide SDS gels at reducing conditions. Protein bands were excised from gels and were in-gel digested for mass spectrometry analysis according to the protocol at http://msf.ucsf.edu/protocols.html. Briefly: gel bands were cut to little pieces, washed, disulfide-bridges were reduced with DTT (dithiothreitol, Sigma-Aldrich), free sulphydrils were alkylated with IAM (iodoacetamide, Sigma-Aldrich) and proteins were digested with trypsin (sequencing grade modified porocine trypsin, Promega) at 37 °C for 4 h. Tryptic peptides were extracted and analysed by MALDI-TOF (Bruker Reflex III) using DHB (2,5 dihydroxybenzoic acid) as matrix, in positive reflectron mode. Peptide sequences were confirmed by MS/MS analysis acquired on a

nanoLC coupled LCQ-Fleet (Thermo Fisher Scientific) ion trap mass spectrometer. To test for correct insertion of the *p*Bpa amino acid into a desired amber codon coded position, we chose position 131 of mPrP and generated two mutants for this position: one coding for a tyrosine [mPrP(S131Y)mCherry] and another for an amber stop codon to initiate insertion of *p*Bpa [mPrP(S131*p*Bpa)mCherry]. The tyrosine mutant serves as a control, given that the tRNA-RNA synthetase pair may preserve some potency for being charged by tyrosine over *p*Bpa. The tyrosine mutant was expressed in two conditions: in LB culture media (-*p*Bpa) or in LB media supplemented with *p*Bpa amino acid (+*p*Bpa). In parallel, the amber codon mutant was expressed in *p*Bpa-supplemented LB media. For a thorough verification of *p*Bpa vs. tyrosine incorporation, mass spectrometry analysis was performed not only on these three protein samples but also on mixtures of purified *p*Bpa- and Tyr-mutant grown in presence of pBpa samples {mPrP(S131Y)mCherry and [mPrP(S131*p*Bpa)mCherry, +*p*Bpa], respectively} containing the two at various percentages, such as: 75:25, 88:12 and 94:6% of *p*Bpa- to Tyr-mutant (Mixture 1-3, respectively, on Fig. S1). MALDI-TOF mass spectrometry analysis of the six samples confirmed that both tyrosine-mutant proteins contained only Tyr at position 131, irrespective of whether the culture media contained *p*Bpa or not, whereas in the *p*Bpa-mutant protein sample only para-benzoyl-phenylalanine could be detected at position 131. In the mixtures of the two proteins, both Tyr and *p*Bpa containing corresponding fragments could be identified with the exception of the third mixture, made up of 94% *p*Bpa-mutant and 6% of Tyr-mutant, where only *p*Bpa-containing corresponding fragments were detected. Based on these we can conclude that a correctly inserted *p*Bpa is present in more than 88% in the produced *p*Bpa-mutant protein samples.

Conformational stability analysis by urea denaturation assay

Conformational stabilities of the wild type and *p*Bpa-mutant prion proteins were compared by using a method based [86], as follows. An urea (Sigma-Aldrich) concentration gradient treatment was applied to the proteins in presence of small amount of reducing agent that can reduce the single disulfide bond present in the structure of the prion protein upon unfolding. Samples of 7.44 µM protein were treated by increasing concentrations of urea, starting from 0 to 5 M in steps of one molar increment, in presence of 20 mM DTT (Sigma-Aldrich) in phosphate buffer saline (PBS), pH 7.4. Treatments were applied for 2.5 h while samples were kept at RT and on a mini-rotator (Bio RS-24 from BioSan, Latvia). After treatment, excess amount (50 mM) of N-Ethylmaleimide (NEM) (Sigma-Aldrich) was added and samples were incubated for additional 1 h to block the reduced thiol groups of the unfolded protein population and DTT. Laemmli SDS sample buffer with no reducing agent was added and samples were tested on 10% SDS-PAGE followed by RAMA staining [104] to visualize the non-reduced and reduced populations present in the protein samples. Since we found that the width of the transition region and midpoint were sensitive to the actual experiment/condition of the protein preparation, for the stability comparisons we performed the assay side-by-side for samples to be compared. Also, we have repeated the unfolding experiments at least on three separate protein preparations.

Photo-crosslinking of PrP dimers

Photo-crosslinking of *p*Bpa-mutant PrP dimers were performed on samples of 6 µM protein in PBS, pH 7.4 buffer containing 0.06% SDS (SERVA) that favored dimerization and crosslinking of dimers at highest amounts (Fig. S3). Volumes of 200 µl sample in 1.5 ml microfuge tubes were placed on ice at a distance of 5 cm from the light bulbs [105] and were irradiated by 365 nm UV light for 2 h to give highest amounts of crosslinked proteins [98] using a Crosslinker CL-1 (Herolab Gmbh, Germany) apparatus, producing a total UV energy

of 18.598 J/cm^2. As negative controls, the wild type proteins containing no *p*Bpa were also included in the experiment. For each sample non-irradiated control pairs were also prepared that were incubated in similar conditions but at dark.

To estimate the amount of the background, non-specifically associated and crosslinked dimers similar experiments were performed with each protein at higher, 2% SDS condition that favors a monomeric form of the prion protein [76]. Above this SDS % the amount of background crosslinked dimers did not decrease anymore (Fig. S5).

Quantification and statistical analysis

Estimation of the dimer-crosslinking efficiencies

Crosslinked samples were tested on either 10% or 12% SDS-PAGE, in case of the mCherry-tagged and untagged mPrP proteins, respectively, followed by RAMA staining (Fig. 3, 4, 7, S6 and S7). The percentage of photo-crosslinked dimer to monomer ratios were assessed by gel-densitometry using the ImageJ 1.48v program [106]. As discussed earlier, in case of the mCherry tagged protiens, the mCherry fusion tag presents cleavage products when incubated/boiled in the sample-buffer that results additional bands below dimer- and monomer-levels on the gel (Fig. 3, 4 and S6). Assuming that the mCherry split occurs the same way in a monomeric or a dimeric (or multimeric) species, the dimer percentage can be calculated using the percent area of the band of dimer considering the areas of the monomeric and dimeric proteins as total (similarly as for the untagged mPrP protein variants). Performing such evaluations for both irradiated and control, non-irradiated (-) samples that were kept at dark and using these latest values for subtractions (for both types of proteins), the crosslinked dimer percentages can be corrected for the “background” fraction of dimers not attributable to UV-crosslinking. The wild type protein samples treated the same way also provide a non-zero

value (perhaps representing dimer products cross-linked at some non-*p*Bpa positions) that was also considered to interpret the *p*Bpa-specific values obtained for the mutants. Similar evaluation of samples at 2% SDS condition was also performed to have an estimate of a (maximum possible) nonspecifically crosslinked dimer amount.

All crosslinking experiments were performed at least on three independent protein samples ($n \geq 3$) originating from different expressions. For data representations the mean ± SD of these values is used. Differences between the values obtained at 0.06% and 2% SDS conditions for each protein examined were tested for significance using unpaired Student's t-test with GraphPad Prism software. Asterisks indicate as follows, *: $p<0.05$, **: $p<0.01$ and ***: $p<0.001$.

Circular dichroism spectroscopy

Far-UV circular dichroic (CD) spectra of samples of the untagged wild type and pBpa-mutant mPrP proteins, typically of 0.1 to 0.2 mg/ml concentrations, were recorded at room temperature using a Jasco J-810 spectropolarimeter, using a 1 mm path length quartz cuvette as the sample holder. CD spectra were recorded between 180 to 260 nm, at 100 nm/min speed, using 2 nm bandwidth and 4 s integration time, sensitivity standard, 1 nm data pitch, and accumulating three spectra for each sample. For each type of protein variant spectra were recorded in three conditions: in the initial conditions of a monomeric-state (in MilliQ water) and in dimer-state favoring conditions of 0.06% SDS, PBS pH 7.2, after either crosslinking by UV light for 2 h or without crosslinking (on parallel samples kept at dark for 2 h). The corresponding buffer-only spectra for each condition and sample were recorded similarly as the sample spectra and were used to subtract from sample spectrum before calculating the mean residue molar ellipticities (degrees square centimeter per decimole). Spectra were

analyzed for secondary structure composition based on Micsonai et al. [107] using the algorithm BeStSel (http://bestsel.elte.hu). Recordings were performed on two to three separate crosslinking experiments.

Acknowledgments

We thank Mária Ádámné-Meszlényi, Papdiné-Morovicz Andrea and Erika Zukic for technical assistance, Ottó Zsíros and Győző Garab for help with CD spectroscopy. The work was supported by the Economic Development and Innovation Operative Programme (EDIOP/GINOP), grant number: GINOP-2.1.7-15-2016-02021.

Author Contributions

E.W. conceived the study; E.W., E.F., S.B.S. designed the experiments; S.B.S. performed protein expression, purification and crosslinking; K.H., P.B., A.N. performed cloning of the DNA-constructs; É.H.-G. performed mass spectrometry analysis. All authors participated in the analysis of the data. E.W., S.B.S., E.F. wrote the manuscript with input from all authors.

Declaration of Interests

The authors declare no competing interests.

References

[1] N. Singh, D. Das, A. Singh, M.L. Mohan, Prion protein and metal interaction: Physiological and pathological implications, Curr. Issues Mol. Biol. 12 (2010) 99–108.

[2] C.L. Haigh, D.R. Brown, Prion protein reduces both oxidative and non-oxidative copper toxicity, J. Neurochem. 98 (2006) 677–689. doi:10.1111/j.1471-4159.2006.03906.x.

[3] W. Rachidi, F. Chimienti, M. Aouffen, A. Senator, P. Guiraud, M. Seve, A. Favier, Prion protein protects against zinc-mediated cytotoxicity by modifying intracellular exchangeable zinc and inducing metallothionein expression, J. Trace Elem. Med. Biol. 23 (2009) 214–223. doi:10.1016/j.jtemb.2009.02.007.

[4] C.J. Choi, V. Anantharam, N.J. Saetveit, R.S. Houk, A. Kanthasamy, A.G. Kanthasamy, Normal cellular prion protein protects against manganese-induced oxidative stress and apoptotic cell death., Toxicol. Sci. 98 (2007) 495–509. doi:10.1093/toxsci/kfm099.

[5] A. Rana, D. Gnaneswari, S. Bansal, B. Kundu, Prion metal interaction: Is prion pathogenesis a cause or a consequence of metal imbalance?, Chem. Biol. Interact. 181 (2009) 282–291. doi:10.1016/j.cbi.2009.07.021.

[6] P.K.R. Cingaram, A. Nyeste, D.T. Dondapati, E. Fodor, E. Welker, Prion protein does not confer resistance to hippocampus-derived Zpl cells against the toxic effects of Cu2+, Mn2+, Zn2+ and Co2+ not supporting a general protective role for PrP in transition metal induced toxicity, PLoS One. 10 (2015) 1–20. doi:10.1371/journal.pone.0139219.

[7] L. Westergard, H.M. Christensen, D.A. Harris, The cellular prion protein (PrP(C)): its physiological function and role in disease., Biochim. Biophys. Acta. 1772 (2007) 629–44. doi:10.1016/j.bbadis.2007.02.011.

[8] R. Linden, V.R. Martins, M. a M. Prado, M. Cammarota, I. Izquierdo, R.R. Brentani, Physiology of the prion protein., Physiol. Rev. 88 (2008) 673–728. doi:10.1152/physrev.00007.2007.

[9] J. Collinge, Prion diseases of humans and animals: their causes and molecular basis., Annu. Rev. Neurosci. 24 (2001) 519–550. doi:10.1146/annurev.neuro.24.1.519.

[10] S.B. Prusiner, Prions, Proc. Natl. Acad. Sci. U. S. A. 95 (1998) 13363. doi:10.1073/pnas.95.23.13363.

[11] A. Aguzzi, M. Polymenidou, Mammalian Prion Biology: One Century of Evolving Concepts, Cell. 116 (2004) 313–327. doi:10.1016/S0092-8674(03)01031-6.

[12] A. Aguzzi, M. Heikenwalder, Pathogenesis of prion diseases: current status and future outlook., Nat. Rev. Microbiol. 4 (2006) 765–775. doi:10.1038/nrmicro1492.

[13] M.A. Baldwin, Mass spectrometric analysis of prion proteins., Adv Protein Chem. 57 (2001) 29–54.

[14] E. Turk, D.B. Teplow, L.E. Hood, S.B. Prusiner, Purification and properties of the cellular and scrapie hamster prion proteins., Eur. J. Biochem. 176 (1988) 21–30. doi:10.1111/j.1432-1033.1988.tb14246.x.

[15] E. Welker, L.D. Raymond, H.A. Scheraga, B. Caughey, Intramolecular versus intermolecular disulfide bonds in prion proteins, J. Biol. Chem. 277 (2002) 33477–33481. doi:10.1074/jbc.M204273200.

[16] D.G. Donne, J.H. Viles, D. Groth, I. Mehlhorn, T.L. James, F.E. Cohen, S.B. Prusiner, P.E. Wright, H.J. Dyson, Structure of the recombinant full-length hamster prion protein PrP(29-231): the N terminus is highly flexible., Proc. Natl. Acad. Sci. U. S. A. 94 (1997) 13452–7. doi:10.1073/pnas.94.25.13452.

[17] T.L. James, H. Liu, N.B. Ulyanov, S. Farr-Jones, H. Zhang, D.G. Donne, K. Kaneko, D. Groth, I. Mehlhorn, S.B. Prusiner, F.E. Cohen, Solution structure of a 142-residue

recombinant prion protein corresponding to the infectious fragment of the scrapie isoform., Proc. Natl. Acad. Sci. U. S. A. 94 (1997) 10086–91. doi:10.1073/pnas.94.19.10086.

[18] R. Riek, S. Hornemann, G. Wider, R. Glockshuber, K. Wüthrich, NMR characterization of the full-length recombinant murine prion protein, mPrP(23-231), FEBS Lett. 413 (1997) 282–288. doi:10.1016/S0014-5793(97)00920-4.

[19] R. Riek, S. Hornemann, G. Wider, M. Billeter, R. Glockshuber, K. Wüthrich, NMR structure of the mouse prion protein domain PrP(121-231)., Nature. 382 (1996) 180–2. doi:10.1038/382180a0.

[20] R. Zahn, A. Liu, T. Lührs, R. Riek, C. von Schroetter, F. López García, M. Billeter, L. Calzolai, G. Wider, K. Wüthrich, NMR solution structure of the human prion protein., Proc. Natl. Acad. Sci. U. S. A. 97 (2000) 145–50. doi:10.1073/pnas.97.1.145.

[21] L.F. Haire, S.M. Whyte, N. Vasisht, A.C. Gill, C. Verma, E.J. Dodson, G.G. Dodson, P.M. Bayley, The Crystal Structure of the Globular Domain of Sheep Prion Protein, J. Mol. Biol. 336 (2004) 1175–1183. doi:10.1016/j.jmb.2003.12.059.

[22] B. Caughey, G.S. Baron, B. Chesebro, M. Jeffrey, Getting a grip on prions: oligomers, amyloids, and pathological membrane interactions., Annu Rev Biochem. 78 (2009) 177–204. doi:10.1146/annurev.biochem.78.082907.145410.

[23] C.J. Silva, E. Vázquez-Fernández, B. Onisko, J.R. Requena, Proteinase K and the structure of PrPSc: The good, the bad and the ugly, Virus Res. 207 (2015) 120–126. doi:10.1016/j.virusres.2015.03.008.

[24] R. Diaz-Espinoza, C. Soto, High-resolution structure of infectious prion protein: the final frontier., Nat. Struct. Mol. Biol. 19 (2012) 370–7. doi:10.1038/nsmb.2266.

[25] C. Govaerts, H. Wille, S.B. Prusiner, F.E. Cohen, Evidence for assembly of prions with left-handed beta-helices into trimers., Proc. Natl. Acad. Sci. U. S. A. 101 (2004) 8342–

8347. doi:10.1073/pnas.0402254101.

[26] B.R. Groveman, M.A. Dolan, L.M. Taubner, A. Kraus, R.B. Wickner, B. Caughey, Parallel in-register intermolecular β-sheet architectures for prion-seeded prion protein (PrP) amyloids, J. Biol. Chem. 289 (2014) 24129–24142. doi:10.1074/jbc.M114.578344.

[27] J.A. Rodriguez, L. Jiang, D.S. Eisenberg, Toward the Atomic Structure of PrP, (2017) 1–18. doi:10.1101/cshperspect.a031336.

[28] M.L. DeMarco, J. Silveira, B. Caughey, V. Daggett, Structural properties of prion protein protofibrils and fibrils: An experimental assessment of atomic models, Biochemistry. 45 (2006) 15573–15582. doi:10.1021/bi0612723.

[29] R.A. Bessen, D.A. Kocisko, G.J. Raymond, S. Nandan, P.T. Lansbury, B. Caughey, Non-genetic propagation of strain-specific properties of scrapie prion protein., Nature. 375 (1995) 698–700. doi:10.1038/375698a0.

[30] J. Castilla, P. Saá, C. Hetz, C. Soto, In vitro generation of infectious scrapie prions, Cell. 121 (2005) 195–206. doi:10.1016/j.cell.2005.02.011.

[31] N.R. Deleault, B.T. Harris, J.R. Rees, S. Supattapone, Formation of native prions from minimal components in vitro., Proc. Natl. Acad. Sci. U. S. A. 104 (2007) 9741–6. doi:10.1073/pnas.0702662104.

[32] M. Horiuchi, S.A. Priola, J. Chabry, B. Caughey, Interactions between heterologous forms of prion protein: Binding, inhibition of conversion, and species barriers, Proc. Natl. Acad. Sci. 97 (2000) 5836–5841. doi:10.1073/pnas.110523897.

[33] J. Il Kim, I. Cali, K. Surewicz, Q. Kong, G.J. Raymond, R. Atarashi, B. Race, L. Qing, P. Gambetti, B. Caughey, W.K. Surewicz, Mammalian prions generated from bacterially expressed prion protein in the absence of any mammalian cofactors, J. Biol. Chem. 285 (2010) 14083–14087. doi:10.1074/jbc.C110.113464.

[34] D. a Kocisko, J.H. Come, S. a Priola, B. Chesebro, G.J. Raymond, P.T. Lansbury, B. Caughey, Cell-free formation of protease-resistant prion protein., Nature. 370 (1994) 471–474. doi:10.1038/370471a0.

[35] G. Legname, I. V Baskakov, H.-O.B. Nguyen, D. Riesner, F.E. Cohen, S.J. DeArmond, S.B. Prusiner, Synthetic mammalian prions., Science. 305 (2004) 673–6. doi:10.1126/science.1100195.

[36] G.P. Saborio, B. Permanne, C. Soto, Sensitive detection of pathological prion protein by cyclic amplification of protein misfolding., Nature. 411 (2001) 810–813. doi:10.1038/35081095.

[37] J. Wang, F.; Wang, Xinhe; Yuan, Chong-Gang; Ma, Generating a Prion with Bacterially Expressed Recombinant Protein, Science (80-.). 327 (2010) 1132–1135. doi:10.1126/science.1183748.

[38] V. Smirnovas, J. Il Kim, X. Lu, R. Atarashi, B. Caughey, W.K. Surewicz, Distinct structures of scrapie prion protein (PrPSc)-seeded versus spontaneous recombinant prion protein fibrils revealed by hydrogen/deuterium exchange, J. Biol. Chem. 284 (2009) 24233–24241. doi:10.1074/jbc.M109.036558.

[39] N. Gonzalez-Montalban, N. Makarava, R. Savtchenko, I. V. Baskakov, Relationship between conformational stability and amplification efficiency of prions, Biochemistry. 50 (2011) 7933–7940. doi:10.1021/bi200950v.

[40] F. Wang, X. Wang, C.D. Orrú, B.R. Groveman, K. Surewicz, R. Abskharon, M. Imamura, T. Yokoyama, Y.S. Kim, K.J. Vander Stel, K. Sinniah, S.A. Priola, W.K. Surewicz, B. Caughey, J. Ma, Self-propagating, protease-resistant, recombinant prion protein conformers with or without in vivo pathogenicity, PLoS Pathog. 13 (2017). doi:10.1371/journal.ppat.1006491.

[41] B.R. Groveman, G.J. Raymond, K.J. Campbell, B. Race, L.D. Raymond, A.G.

Hughson, C.D. Orrú, A. Kraus, K. Phillips, B. Caughey, Role of the central lysine cluster and scrapie templating in the transmissibility of synthetic prion protein aggregates, PLoS Pathog. 13 (2017). doi:10.1371/journal.ppat.1006623.

[42] N. Makarava, R. Savtchenko, I. V. Baskakov, Methods of protein misfolding cyclic amplification, in: Methods Mol. Biol., 2017: pp. 169–183. doi:10.1007/978-1-4939-7244-9_13.

[43] A. Kraus, G.J. Raymond, B. Race, K.J. Campbell, A.G. Hughson, K.J. Anson, L.D. Raymond, B. Caughey, PrP P102L and Nearby Lysine Mutations Promote Spontaneous *In Vitro* Formation of Transmissible Prions, J. Virol. 91 (2017) e01276-17. doi:10.1128/JVI.01276-17.

[44] S. Liemann, R. Glockshuber, Influence of amino acid substitutions related to inherited human prion diseases on the thermodynamic stability of the cellular prion protein., Biochemistry. 38 (1999) 3258–67. doi:10.1021/bi982714g.

[45] W. Swietnicki, R.B. Petersen, P. Gambetti, W.K. Surewicz, Familial Mutations and the Thermodynamic Stability of the Recombinant Human Prion Protein, J. Biol. Chem. 273 (1998) 31048–31052. doi:10.1074/jbc.273.47.31048.

[46] I. V. Baskakov, G. Legname, M.A. Baldwin, S.B. Prusiner, F.E. Cohen, Pathway complexity of prion protein assembly into amyloid, J. Biol. Chem. 277 (2002) 21140–21148. doi:10.1074/jbc.M111402200.

[47] S. Jain, J.B. Udgaonkar, Evidence for Stepwise Formation of Amyloid Fibrils by the Mouse Prion Protein, J. Mol. Biol. 382 (2008) 1228–1241. doi:10.1016/j.jmb.2008.07.052.

[48] S. Jain, J.B. Udgaonkar, Salt-induced modulation of the pathway of amyloid fibril formation by the mouse prion protein, Biochemistry. 49 (2010) 7615–7624. doi:10.1021/bi100745j.

[49] L.L.P. Hosszu, C.R. Trevitt, S. Jones, M. Batchelor, D.J. Scott, G.S. Jackson, J. Collinge, J.P. Waltho, A.R. Clarke, Conformational properties of β-PrP, J. Biol. Chem. 284 (2009) 21981–21990. doi:10.1074/jbc.M809173200.

[50] F. Eghiaian, T. Daubenfeld, Y. Quenet, M. van Audenhaege, A.-P.P. Bouin, G. van der Rest, J. Grosclaude, H. Rezaei, Diversity in prion protein oligomerization pathways results from domain expansion as revealed by hydrogen/deuterium exchange and disulfide linkage., Proc. Natl. Acad. Sci. U. S. A. 104 (2007) 7414–7419. doi:10.1073/pnas.0607745104.

[51] C. Wong, L.W. Xiong, M. Horiuchi, L. Raymond, K. Wehrly, B. Chesebro, B. Caughey, Sulfated glycans and elevated temperature stimulate PrPsc-dependent cell-free formation of protease-resistant prion protein, EMBO J. 20 (2001) 377–386. doi:10.1093/emboj/20.3.377.

[52] L. Breydo, N. Makarava, I. V. Baskakov, Methods for conversion of prion protein into amyloid fibrils, Methods Mol. Biol. 459 (2008) 105–115. doi:10.1007/978-1-59745-234-2-8.

[53] G.S. Jackson, A.F. Hill, C. Joseph, L. Hosszu, A. Power, J.P. Waltho, A.R. Clarke, J. Collinge, Multiple folding pathways for heterologously expressed human prion protein., Biochim. Biophys. Acta. 1431 (1999) 1–13.

[54] G.S. Jackson, L.L. Hosszu, A. Power, A.F. Hill, J. Kenney, H. Saibil, C.J. Craven, J.P. Waltho, A.R. Clarke, J. Collinge, Reversible conversion of monomeric human prion protein between native and fibrilogenic conformations., Science. 283 (1999) 1935–7. doi:10.1126/science.283.5409.1935.

[55] H. Zhang, J. Stockel, I. Mehlhorn, D. Groth, M.A. Baldwin, S.B. Prusiner, T.L. James, F.E. Cohen, Physical studies of conformational plasticity in a recombinant prion protein., Biochemistry. 36 (1997) 3543–53. doi:10.1021/bi961965r.

[56] N. Klimova, N. Makarava, I. V. Baskakov, The diversity and relationship of prion protein self-replicating states, Virus Res. 207 (2015) 113–119. doi:10.1016/j.virusres.2014.10.002.

[57] D.B.D. O'Sullivan, C.E. Jones, S.R. Abdelraheim, A.R. Thompsett, M.W. Brazier, H. Toms, D.R. Brown, J.H. Viles, NMR characterization of the pH 4 beta-intermediate of the prion protein: the N-terminal half of the protein remains unstructured and retains a high degree of flexibility., Biochem. J. 401 (2007) 533–40. doi:10.1042/BJ20060668.

[58] K. Schlepckow, H. Schwalbe, Molecular mechanism of prion protein oligomerization at atomic resolution, Angew. Chemie - Int. Ed. 52 (2013) 10002–10005. doi:10.1002/anie.201305184.

[59] J. Singh, J.B. Udgaonkar, Dissection of conformational conversion events during prion amyloid fibril formation using hydrogen exchange and mass spectrometry, J. Mol. Biol. 425 (2013) 3510–3521. doi:10.1016/j.jmb.2013.06.009.

[60] J. Singh, A.T. Sabareesan, M.K. Mathew, J.B. Udgaonkar, Development of the structural core and of conformational heterogeneity during the conversion of oligomers of the mouse prion protein to worm-like amyloid fibrils, J. Mol. Biol. 423 (2012) 217–231. doi:10.1016/j.jmb.2012.06.040.

[61] N. Makarava, I. V. Baskakov, The same primary structure of the prion protein yields two distinct self-propagating states, J. Biol. Chem. 283 (2008) 15988–15996. doi:10.1074/jbc.M800562200.

[62] Z.E. Arellano Anaya, J. Savistchenko, V. Massonneau, C. Lacroux, O. Andréoletti, D. Vilette, Recovery of small infectious PrPres aggregates from prion-infected cultured cells, J. Biol. Chem. 286 (2011) 8141–8148. doi:10.1074/jbc.M110.165233.

[63] N. Sanghera, M. Wall, C. Vénien-Bryan, T.J.T. Pinheiro, Globular and pre-fibrillar prion aggregates are toxic to neuronal cells and perturb their electrophysiology,

Biochim. Biophys. Acta - Proteins Proteomics. 1784 (2008) 873–881. doi:10.1016/j.bbapap.2008.02.017.

[64] C. Hundt, S. Gauczynski, C. Leucht, M.L. Riley, S. Weiss, Intra- and interspecies interactions between prion proteins and effects of mutations and polymorphisms., Biol. Chem. 384 (2003) 791–803. doi:10.1515/BC.2003.088.

[65] R.K. Meyer, A. Lustig, B. Oesch, R. Fatzer, A. Zurbriggen, M. Vandevelde, A Monomer-Dimer Equilibrium of a Cellular Prion Protein (PrPC) Not Observed with Recombinant PrP, J. Biol. Chem. 275 (2000) 38081–38087. doi:10.1074/jbc.M007114200.

[66] S.A. Priola, B. Caughey, K. Wehrly, B. Chesebro, A 60-kDa prion protein (PrP) with properties of both the normal and scrapie-associated forms of PrP., J. Biol. Chem. 270 (1995) 3299–305.

[67] A.S. Rambold, V. Müller, U. Ron, N. Ben-Tal, K.F. Winklhofer, J. Tatzelt, Stress-protective signalling of prion protein is corrupted by scrapie prions, EMBO J. 27 (2008) 1974–1984. doi:10.1038/emboj.2008.122.

[68] X. Roucou, Regulation of PrP(C) signaling and processing by dimerization., Front. Cell Dev. Biol. 2 (2014) 57. doi:10.3389/fcell.2014.00057.

[69] U.K. Resenberger, A. Harmeier, A.C. Woerner, J.L. Goodman, V. Müller, R. Krishnan, R.M. Vabulas, H.A. Kretzschmar, S. Lindquist, F.U. Hartl, G. Multhaup, K.F. Winklhofer, J. Tatzelt, The cellular prion protein mediates neurotoxic signalling of β-sheet-rich conformers independent of prion replication., EMBO J. 30 (2011) 2057–70. doi:10.1038/emboj.2011.86.

[70] B.R. Fluharty, E. Biasini, M. Stravalaci, A. Sclip, L. Diomede, C. Balducci, P. La Vitola, M. Messa, L. Colombo, G. Forloni, T. Borsello, M. Gobbi, D.A. Harris, An N-terminal fragment of the prion protein binds to amyloid-β oligomers and inhibits their

neurotoxicity in vivo., J. Biol. Chem. 288 (2013) 7857–66. doi:10.1074/jbc.M112.423954.

[71] L. Westergard, J.A. Turnbaugh, D.A. Harris, A naturally occurring C-terminal fragment of the prion protein (PrP) delays disease and acts as a dominant-negative inhibitor of PrPSc formation., J. Biol. Chem. 286 (2011) 44234–42. doi:10.1074/jbc.M111.286195.

[72] M. Beland, J. Motard, A. Barbarin, X. Roucou, PrPC Homodimerization Stimulates the Production of PrPC Cleaved Fragments PrPN1 and PrPC1, J. Neurosci. 32 (2012) 13255–13263. doi:10.1523/JNEUROSCI.2236-12.2012.

[73] M. Béland, X. Roucou, Homodimerization as a molecular switch between low and high efficiency PrP C cell surface delivery and neuroprotective activity., Prion. 7 (2013) 170–4. doi:10.4161/pri.23583.

[74] J.B. Oliveira-Martins, S. Yusa, A.M. Calella, C. Bridel, F. Baumann, P. Dametto, A. Aguzzi, Unexpected tolerance of alpha-cleavage of the prion protein to sequence variations., PLoS One. 5 (2010) e9107. doi:10.1371/journal.pone.0009107.

[75] K. Jansen, O. Schäfer, E. Birkmann, K. Post, H. Serban, S.B. Prusiner, D. Riesner, Structural intermediates in the putative pathway from the cellular prion protein to the pathogenic form, Biol. Chem. 382 (2001) 683–691. doi:10.1515/BC.2001.081.

[76] T. Kaimann, S. Metzger, K. Kuhlmann, B. Brandt, E. Birkmann, H.D. Höltje, D. Riesner, Molecular Model of an α-Helical Prion Protein Dimer and Its Monomeric Subunits as Derived from Chemical Cross-linking and Molecular Modeling Calculations, J. Mol. Biol. 376 (2008) 582–596. doi:10.1016/j.jmb.2007.11.035.

[77] J. Stöhr, N. Weinmann, H. Wille, T. Kaimann, L. Nagel-Steger, E. Birkmann, G. Panza, S.B. Prusiner, M. Eigen, D. Riesner, Mechanisms of prion protein assembly into amyloid., Proc. Natl. Acad. Sci. U. S. A. 105 (2008) 2409–14.

doi:10.1073/pnas.0712036105.

[78] Y. Ryu, P.G. Schultz, Efficient incorporation of unnatural amino acids into proteins in Escherichia coli., Nat. Methods. 3 (2006) 263–5. doi:10.1038/nmeth864.

[79] E. Biasini, L. Tapella, E. Restelli, M. Pozzoli, T. Massignan, R. Chiesa, The hydrophobic core region governs mutant prion protein aggregation and intracellular retention., Biochem. J. 430 (2010) 477–486. doi:10.1042/BJ20100615.

[80] A. Li, H.M. Christensen, L.R. Stewart, K. a Roth, R. Chiesa, D. a Harris, Neonatal lethality in transgenic mice expressing prion protein with a deletion of residues 105-125., EMBO J. 26 (2007) 548–58. doi:10.1038/sj.emboj.7601507.

[81] D. Peretz, R. a Williamson, Y. Matsunaga, H. Serban, C. Pinilla, R.B. Bastidas, R. Rozenshteyn, T.L. James, R. a Houghten, F.E. Cohen, S.B. Prusiner, D.R. Burton, A conformational transition at the N terminus of the prion protein features in formation of the scrapie isoform., J. Mol. Biol. 273 (1997) 614–622. doi:10.1006/jmbi.1997.1328.

[82] J. Hendrix, C. Flors, P. Dedecker, J. Hofkens, Y. Engelborghs, Dark States in Monomeric Red Fluorescent Proteins Studied by Fluorescence Correlation and Single Molecule Spectroscopy, Biophys. J. 94 (2008) 4103–4113. doi:10.1529/biophysj.107.123596.

[83] R.E. Campbell, R.E. Campbell, O. Tour, O. Tour, A.E. Palmer, A.E. Palmer, P. a Steinbach, P. a Steinbach, G.S. Baird, G.S. Baird, D. a Zacharias, D. a Zacharias, R.Y. Tsien, R.Y. Tsien, A monomeric red fluorescent protein., Proc. Natl. Acad. Sci. U. S. A. 99 (2002) 7877–82. doi:10.1073/pnas.082243699.

[84] V. V. Verkhusha, A. Sorkin, Conversion of the monomeric red fluorescent protein into a photoactivatable probe, Chem. Biol. 12 (2005) 279–285. doi:10.1016/j.chembiol.2005.01.005.

[85] L.A. Gross, G.S. Baird, R.C. Hoffman, K.K. Baldridge, R.Y. Tsien, The structure of

the chromophore within DsRed, a red fluorescent protein from coral, Proc. Natl. Acad. Sci. 97 (2000) 11990–11995. doi:10.1073/pnas.97.22.11990.

[86] G. Xu, M. Narayan, E. Welker, H.A. Scheraga, A novel method to determine thermal transition curves of disulfide-containing proteins and their structured folding intermediates, Biochem. Biophys. Res. Commun. 311 (2003) 514–517. doi:10.1016/j.bbrc.2003.10.039.

[87] L. Calzolai, D.A. Lysek, P. Guntert, C. von Schroetter, R. Riek, R. Zahn, K. Wüthrich, NMR structures of three single-residue variants of the human prion protein., Proc. Natl. Acad. Sci. U. S. A. 97 (2000) 8340–5. doi:10.1073/pnas.97.15.8340.

[88] F. López Garcia, R. Zahn, R. Riek, K. Wüthrich, NMR structure of the bovine prion protein., Proc. Natl. Acad. Sci. U. S. A. 97 (2000) 8334–9. doi:10.1073/pnas.97.15.8334.

[89] R. Linden, V.R. Martins, M. a M. Prado, M. Cammarota, I. Izquierdo, R.R. Brentani, A. Aguzzi, A.M. Calella, B. Chesebro, A. Aguzzi, M. Polymenidou, S.B. Prusiner, J. Collinge, Prions: protein aggregation and infectious diseases., Physiol. Rev. 88 (2008) 673–728. doi:10.1152/physrev.00006.2009.

[90] J. Singh, H. Kumar, A.T. Sabareesan, J.B. Udgaonkar, Rational stabilization of helix 2 of the prion protein prevents its misfolding and oligomerization, J. Am. Chem. Soc. 136 (2014) 16704–16707. doi:10.1021/ja510964t.

[91] F. Sokolowski, A.J. Modler, R. Masuch, D. Zirwer, M. Baier, G. Lutsch, D.A. Moss, K. Gast, D. Naumann, Formation of Critical Oligomers Is a Key Event during Conformational Transition of Recombinant Syrian Hamster Prion Protein, J. Biol. Chem. 278 (2003) 40481–40492. doi:10.1074/jbc.M304391200.

[92] E. Deseke, Y. Nakatani, G. Ourisson, Intrinsic reactivities of amino acids towards photoalkylation with benzophenone - A study preliminary to photolabelling of the

transmembrane protein glycophorin A, European J. Org. Chem. (1998) 243–251. doi:10.1002/(SICI)1099-0690(199802)1998:2<243::AID-EJOC243>3.0.CO;2-I.

[93] A. Wittelsberger, B.E. Thomas, D.F. Mierke, M. Rosenblatt, Methionine acts as a "magnet" in photoaffinity crosslinking experiments, FEBS Lett. 580 (2006) 1872–1876. doi:10.1016/j.febslet.2006.02.050.

[94] J.K. Lancia, A. Nwokoye, A. Dugan, C. Joiner, R. Pricer, A.K. Mapp, Sequence context and crosslinking mechanism affect the efficiency of in vivo capture of a protein-protein interaction., Biopolymers. 101 (2014) 391–7. doi:10.1002/bip.22395.

[95] R. Atarashi, V.L. Sim, N. Nishida, B. Caughey, S. Katamine, Prion Strain-Dependent Differences in Conversion of Mutant Prion Proteins in Cell Culture, J. Virol. 80 (2006) 7854–7862. doi:10.1128/JVI.00424-06.

[96] R.J. Kascsak, R. Rubenstein, P.A. Merz, M. Tonna-DeMasi, R. Fersko, R.I. Carp, H.M. Wisniewski, H. Diringer, Mouse polyclonal and monoclonal antibody to scrapie-associated fibril proteins., J. Virol. 61 (1987) 3688–93. http://www.pubmedcentral.nih.gov/articlerender.fcgi?artid=255980&tool=pmcentrez&rendertype=abstract.

[97] S. Hornemann, C. Korth, B. Oesch, R. Riek, G. Wider, K. Wüthrich, R. Glockshuber, Recombinant full-length murine prion protein, mPrP(23-231): Purification and spectroscopic characterization, FEBS Lett. 413 (1997) 277–281. doi:10.1016/S0014-5793(97)00921-6.

[98] I.S. Farrell, R. Toroney, J.L. Hazen, R.A. Mehl, J.W. Chin, Photo-cross-linking interacting proteins with a genetically encoded benzophenone., Nat. Methods. 2 (2005) 377–384. doi:10.1038/nmeth0505-377.

[99] T.S. Young, I. Ahmad, J.A. Yin, P.G. Schultz, An Enhanced System for Unnatural Amino Acid Mutagenesis in E. coli, J. Mol. Biol. 395 (2010) 361–374.

doi:10.1016/j.jmb.2009.10.030.

[100] J. F. Sambrook and D.W. Russell, Molecular cloning: A Laboratory Manual.3rd Ed. Vol.1., Cold Spring Harb. Lab. Press. New York, USA. (2001).

[101] B.Y. Lu, P.J. Beck, J.Y. Chang, Oxidative folding of murine prion mPrP(23-231), Eur. J. Biochem. 268 (2001) 3767–3773.

[102] M.M. Lyles, H.F. Gilbert, Catalysis of the oxidative folding of ribonuclease A by protein disulfide isomerase: dependence of the rate on the composition of the redox buffer., Biochemistry. 30 (1991) 613–619. doi:10.1021/bi00217a005.

[103] M.M. Bradford, A rapid and sensitive method for the quantitation of microgram quantities of protein utilizing the principle of protein-dye binding, Anal. Biochem. 72 (1976) 248–254. doi:10.1016/0003-2697(76)90527-3.

[104] H. Yasumitsu, Y. Ozeki, S.M.A. Kawsar, Y. Fujii, M. Sakagami, Y. Matuo, T. Toda, H. Katsuno, RAMA stain: A fast, sensitive and less protein-modifying CBB R250 stain, Electrophoresis. 31 (2010) 1913–1917. doi:10.1002/elps.200900524.

[105] R. Ahrends, J. Kosinski, D. Kirsch, L. Manelyte, L. Giron-Monzon, L. Hummerich, O. Schulz, B. Spengler, P. Friedhoff, Identifying an interaction site between MutH and the C-terminal domain of MutL by crosslinking, affinity purification, chemical coding and mass spectrometry, Nucleic Acids Res. 34 (2006) 3169–3180. doi:10.1093/nar/gkl407.

[106] W. Rasband, ImageJ [Software], U. S. Natl. Institutes Heal. Bethesda, Maryland, USA. (2015) //imagej.nih.gov/ij/.

[107] A. Micsonai, F. Wien, L. Kernya, Y.H. Lee, Y. Goto, M. Refregiers, J. Kardos, Accurate secondary structure prediction and fold recognition for circular dichroism spectroscopy, PNAS. 112 (2015) E3095–E3103. doi:10.1073/pnas.1500851112.

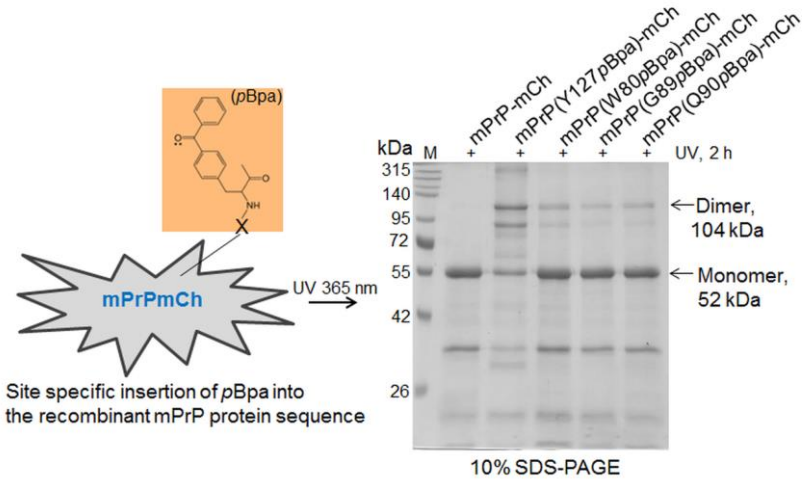

Graphical abstract

Highlights

- The transition of monomeric PrP^{C} to oligomeric PrP^{Sc} is the key event of TSE.
- Over 25 site-specific *p*-benzoyl-L-phenylalanine mutants were used to interrogate the dimeric interface of PrP.
- The N-terminal part of PrP is integral part of the dimer interface.
- These prion-variants may facilitate studying various oligomeric/fibrillar PrP structures.